# Molecular dynamics simulations of fluorine molecules interacting with a Si{100}(2×1) surface at 1000 K

T. A. Schoolcraft[a] and A. M. Diehl
*Department of Chemistry, Shippensburg University, Shippensburg, Pennsylvania 17257*

A. B. Steel[b]
*Department of Chemistry, Gettysburg College, Gettysburg, Pennsylvania 17325*

B. J. Garrison[c]
*Department of Chemistry, The Pennsylvania State University, University Park, Pennsylvania 16802*

(Received 22 April 1994; accepted 11 March 1995)

Molecular dynamics simulations are performed to examine the adsorption of fluorine molecules, having incident translational kinetic energies between 0.0195 and 1.67 eV, on a clean Si{100}(2×1) surface at 1000 K. Results using the Stillinger and Weber potential energy function and the Weakliem, Wu, and Carter parameterization of this potential energy function are compared to each other and to experimental results. The initial sticking probability increases as the incident kinetic energy increases. As the incident kinetic energy increases, more difluorination and less monofluorination is observed as barriers to adsorption are overcome. For difluorination, a time delay between the two atom adsorption events is quantified.

## I. INTRODUCTION

The adsorption of fluorine molecules on a clean Si{100}(2×1) surface is fundamentally different from the adsorption of fluorine atoms. In progressing from atomic fluorine to molecular fluorine, the addition of only one more atom and thus a bond, increases the number of possible reaction results. When fluorine atoms interact with the clean Si{100}(2×1) surface, the atoms can be either repelled or adsorbed.[1] When $F_2$ molecules interact with the clean silicon surface, there are three possible results.[2–5] In one case, the $F_2$ molecule repels from the surface, i.e., no chemical reaction occurs. Another possible result is for the F–F bond to break and one Si–F bond to form with the other fluorine atom ejecting into the vacuum, i.e., monofluorination or atom abstraction. The possible final outcome is for the F–F bond to break and two Si–F bonds to form, i.e., difluorination. Difluorination, generically known as dissociative chemisorption, is generally believed to occur via one of two mechanisms.[6] The first mechanism is direct adsorption. When the $F_2$ molecule adsorbs, the F–F bond breaks immediately upon the molecule's interaction with the surface and two Si–F bonds form. As the incident kinetic energy increases, this mechanism is characterized by an initial sticking probability that increases because it is easier for the activation barrier to be overcome. The second mechanism involves a molecular precursor state. Here the F–F bond does not break immediately upon the molecule's initial interaction with the surface. The molecule loses sufficient translational kinetic energy and becomes physisorbed to the surface. The physisorbed molecule then reorients or diffuses in order to find a site where it can dissociate and therefore chemisorb. The molecule can also fail to react after spending some time physisorbed and then desorb unreacted. The precursor mechanism is characterized by an initial sticking probability that decreases as the incident kinetic energy increases because the molecule must lose more translational energy in order to become trapped. From this study, however, a fourth mechanism for dissociative chemisorption is found that will be referred to as an atomic precursor state mechanism to distinguish it from the molecular precursor state mechanism. In this scenario, one fluorine atom of the $F_2$ molecule chemisorbs, yet the second fluorine atom does not adsorb or desorb immediately. The F–F bond lengthens and the second fluorine atom reorients or diffuses in order to find an adsorption site. If the second fluorine atom finds a dangling bond, the end result is difluorination and, if not, the end result is monofluorination.

Evidence of an atomic precursor state mechanism for the dissociative chemisorption of $F_2$ molecules on the Si{100}(2×1) surface is suggested in theoretical investigations that examine this system,[2,3,7] and also by several experimental investigations that examine the desorption of $H_2$ molecules from the Si{100}(2×1) surface.[8–10] The first theoretical investigation is a molecular dynamics simulation performed by Weber and Stillinger.[2] The authors investigated the reaction dynamics of $F_2$ molecules with a Si{100}(2×1) surface at 0 K. Although Weber and Stillinger display trajectories where the fluorine atoms adsorb nonsimultaneously, they do not investigate them in detail. Provided that this is not an artifact of the potential energy function, the time-staggered adsorption suggests an atomic precursor state mechanism. The second theoretical investigation is a SLAB-MINDO semi-empirical calculation performed by Craig and Smith.[7] These authors found a complexed structure when they examined the minimized energy configuration for an adsorbed $F_2$ molecule on the Si{100}(2×1) surface. The Si–Si dimer bond is stretched from its equilibrium length of 2.217 to 2.859 Å and the F–F bond distance is also stretched from an equilibrium value of 1.446 to 1.610 Å. The $F_2$ molecule is positioned over one end of the dimer pair so that one

---

[a] Electronic mail: TASCHO@ark.ship.edu

[b] Current address: Department of Chemistry, University of Maryland, College Park, MD 20742.

[c] Electronic mail: bjg@chem.psu.edu

fluorine atom is almost vertical above a silicon atom and the other fluorine atom is almost directly above the dimer bridge site. The Si–F bond lengths are 1.615 and 1.618 Å. Although this configuration differs from the Si–F⋯F complex formation observed by Weber and Stillinger,[2] it also suggests a precursor structure to adsorption. Additional support is found in molecular hydrogen desorption studies.[8,9] After several investigations, the unusual first-order recombinative behavior of hydrogen desorption from the Si{100}(2×1) surface was explained as being due to preferential pairing of the hydrogen adatoms on the surface.[10–12] In order for $H_2$ to desorb, each silicon of a dimer pair must be a monohydride species. Next, one hydrogen of the pair migrates toward the other monohydride species to form a dihydride species. Once this species is formed, the $H_2$ desorbs leaving behind an unoccupied dimer pair. This desorption behavior explains the low initial reaction probability of $H_2$ with the Si{100}(2×1) surface. Only silicon atoms which have two dangling bonds can be adsorption sites and these sites are not very numerous on this surface.

The silicon/fluorine potential energy function was developed by Stillinger and Weber (SW).[2,13–15] Weakliem, Wu, and Carter (WWC), finding the Stillinger and Weber potential to be too repulsive for fluorine atom adsorption on the Si{100}(2×1) surface, have reparameterized only the Si–F portion to fit electronic structure calculations of fluorine atom adsorption on Si{100}(2×1).[16,17] These researchers have performed similar calculations as Stillinger and Weber for a 298 K surface instead of a 0 K surface using both the SW potential and the WWC parameterization.[3,18] Since the experimental investigations by Ceyer and co-workers[5] were performed at 1000 K, this article re-examines the reaction pathways of this system at this experimental temperature using the SW potential and WWC parameterization.

## II. DESCRIPTION OF THE SIMULATION

Molecular dynamics calculations are performed for the scattering of $F_2$ molecules from a clean Si{100}(2×1) surface maintained at 1000 K using both the SW silicon/fluorine potential and the WWC parameterization. The temperature of 1000 K is chosen as the experiments of Ceyer *et al.* were performed at this temperature.[5] The silicon crystal consists of 320 atoms where the details of this crystal are described elsewhere in an article describing the spontaneous etching of Si by reaction with F atoms.[19] For the purpose of investigating the dependence of the sticking probability on the incident kinetic energy of the $F_2$ molecule, three different kinetic energies for the fluorine molecules are used: 0.0195, 0.234, and 1.67 eV. The energy of 0.234 eV or 5.4 kcal/mol is the same as used in the simulations at the lower surface temperatures.[2,3] For each incident kinetic energy, 200 trajectories are performed.

To simplify the analysis of a trajectory, the fluorine molecule possesses neither rotational nor vibrational energy, thus all incident kinetic energy is purely translational. The center of mass of the molecule is normally incident and is aimed in a region on the surface that represents the entire surface due to symmetry.[1] The height, $z$, of the center of mass is initially 4.7 Å above the surface. This height places the fluorine molecule sufficiently out of range of any interaction with the surface. Before each deposition event, the crystal's motion is integrated for a random time interval between zero and ~1250 fs ($1\ \mathrm{fs}=1\times10^{-15}$ s), thus allowing the crystal to be in a random vibrational phase for each trajectory of the incoming fluorine molecule. The orientation of the molecule is generated randomly where the azimuthal angle, $\Phi$, is chosen between 0° and 180°, and the polar angle, $\Theta$, is chosen such that cosine $\Theta$ is between 0 and 1.[20]

TABLE I. The number of different trajectory classifications for parameterization and for each incident kinetic energy.

| | 0.0195 eV | | 0.234 eV | | 1.67 eV | |
|---|---|---|---|---|---|---|
| | WWC | SW | WWC | SW | WWC | SW |
| Difluorination | 45 | 34 | 103 | 57 | 172 | 112 |
| Monofluorination | 155 | 140 | 97 | 139 | 28 | 83 |
| Nonreactive | 0 | 19 | 0 | 3 | 0 | 5 |
| Complex | 0 | 7 | 0 | 1 | 0 | 0 |
| $S_0$ | 0.61 | 0.54 | 0.76 | 0.64 | 0.93 | 0.77 |

The result of each trajectory is placed into one of the four categories first observed by Weber and Stillinger:[2] difluorination, monofluorination or atom abstraction, repulsion and complex formation. Difluorination is determined when the total energy of each fluorine atom is $\sim -5$ eV. This indicates that two Si–F bonds have formed since the Si–F bond energy is ~5–7 eV depending upon the parameters in the potential. For comparison, the F–F bond energy is ~1.6 eV and the Si–Si bond energy is ~2–3 eV. Monofluorination is determined when the total energy of one of the fluorine atoms is $\sim -5$ eV, and the potential energy of the other fluorine atom is zero and its $z$ component of the velocity is directed away from the surface. Repulsion is determined when the $z$ coordinate of both of the fluorine atoms passes a plane ~8.4 Å above the surface, the $z$ components of both velocity vectors are directed away from the surface, and the fluorine atoms still form a molecule. Complex formation is defined when the total energy of one fluorine atom is $\sim -5$ eV, the total energy of the other fluorine atom is between $-1$ eV and zero, and ~5 picoseconds (ps) have passed in the simulation. No trajectories formed complexes with the WWC parameterization using 5 ps as a cutoff time to end a trajectory, unlike trajectories calculated using the SW potential. We did not observe trajectories in which both F atoms desorbed as atoms.

## III. RESULTS AND DISCUSSION

The number of each different type of trajectory (difluorination, monofluorination, nonreactive and complex formation) for each parameterization and for each incident kinetic energy is summarized in Table I. At all incident energies the major reaction channels are difluorination and monofluorination with difluorination more predominant at the higher kinetic energies. For the SW potential there are a small amount of trajectories which do not react and a few trajectories in which complexes are formed. In contrast, the simulations at lower temperatures[2,3] have much larger percentages of trajectories (6%–13% at 0.234 eV) in which there is complex

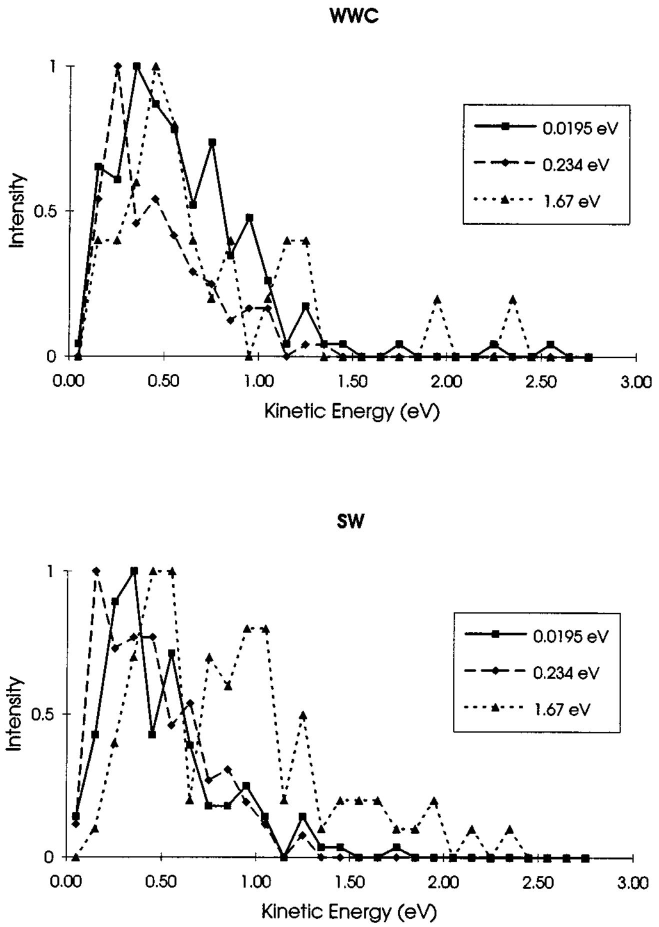

FIG. 1. Kinetic energy distribution of the ejected fluorine atoms for monofluorination events. The distributions are individually peak normalized.

formation, an observation independent of parameterization. For the lower surface temperature the SW potential predicts nonreactive yields of 16%–45%, a value considerably higher than found in these investigations. Likewise, the lower surface temperature simulations show a lower percentage of difluorination relative to monofluorination trajectories. In summary, the higher surface temperature almost eliminates nonreactive and complex formation events. It also enhances difluorination relative to monofluorination.

The two experimental values of the initial sticking probability are by Engstrom *et al.*[21] and Ceyer *et al.*[5] Engstrom reports a value of 0.46 with Ceyer's value approximately 0.83. In the calculations the initial sticking probability, $S_0$, is determined by multiplying the number of difluorination trajectories by two and adding this number to the number of monofluorination and complex formation trajectories and then dividing this sum by twice the total number of trajectories. Since Ceyer's experiments are performed at energies nearer the lower two energy values given in Table I, it appears that the calculated sticking probabilities fall midway between the experimental values. The disturbing feature is that Ceyer finds that the majority (~90%)[5] of the sticking events are difluorination, whereas both the SW potential and the WWC parameterization underestimate the amount of difluorination. Two possibilities for the discrepancy come to mind. First, the activation energy for difluorination could be too large since the Si–F–F interaction is too repulsive.[3] Second, the potential should be longer ranged. This potential and most others for Si are limited to nearest-neighbor interactions. If the real interaction is longer ranged then, after the first fluorination event, the second F atom would be pulled closer to the surface.

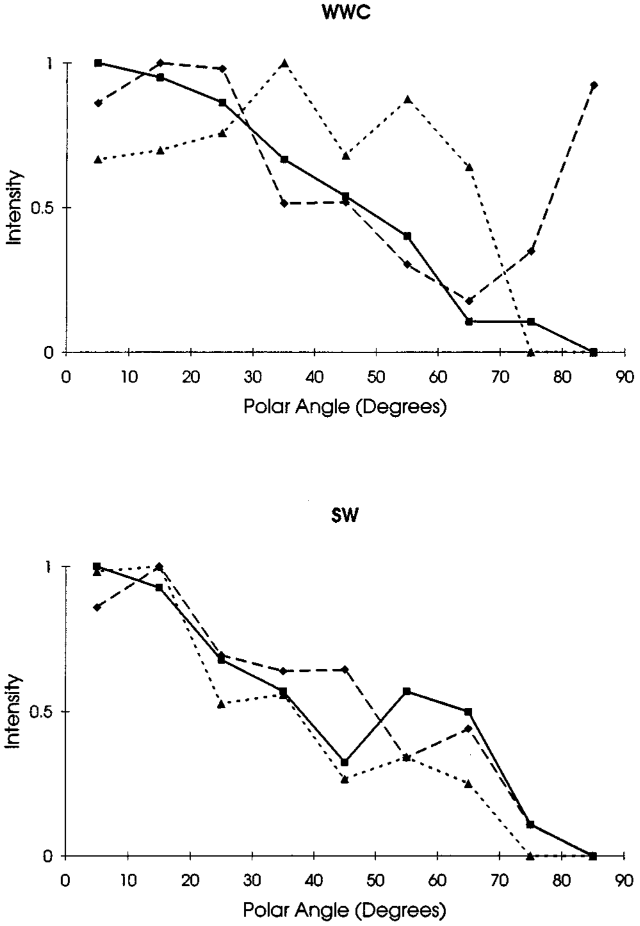

FIG. 2. Polar angle of the ejecting fluorine atom for monofluorination events where 0° is ejection perpendicular to the surface plane and 90° is ejection parallel to the surface plane. The distributions are counted in steps of 10°, are weighted for hemispherical collection, and are peak normalized. The legend is the same as in Fig. 1.

The ejected fluorine atoms from the monofluorinated events are analyzed as to their kinetic energy of ejection (Fig. 1) and their polar angle of ejection (Fig. 2). One striking observation in the kinetic energy distributions is that the shapes of the distributions are similar, i.e., the distributions are not strongly dependent on the initial conditions or parameterization and thus must be a function of the adsorption process. Another observation is that the distributions peak in roughly the same kinetic energy range, 0.25–0.45 eV, even though two of the three incident kinetic energies are below these peak values. Carter *et al.* also observe these same results with a 298 K crystal.[3] Interestingly, the shapes of the polar distributions (Fig. 2) are similar to each other also and are almost "cosine-like," thus, there is no preferred angle of ejection. Once again, this indicates that the atom abstraction event is independent of the initial conditions of the fluorine molecule.

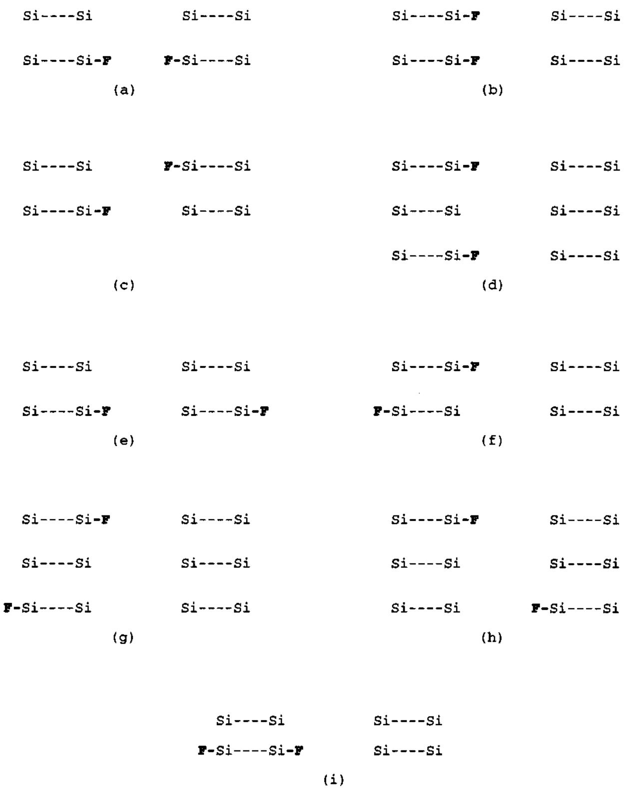

FIG. 3. Difluorination patterns: (a) opposing, (b) vicinal, (c) diagonal, (d) vicinal once-removed, (e) opposing once-removed, (f) diagonal along the row, (g) diagonal along the row once-removed, (h) diagonal across the trough once-removed, and (i) same dimer pair.

The trajectories where both fluorine atoms adsorb to silicon dimer atoms are analyzed as to the patterns of adsorption that result on the surface (Fig. 3) and the probability of adsorption (Tables II and III). Where appropriate, the results in this section are compared to the molecular dynamics results of Weber and Stillinger with a 0 K crystal[2] and to the results of Carter *et al.* with a 298 K crystal.[3] Figures 3(a)–3(i) depict nine of the 11 observed difluorination patterns that are observed in the simulation where the first three patterns are also those observed by Weber and Stillinger. Two patterns not depicted are the formation of an $SiF_2$ adspecies where both fluorine atoms adsorb to the same silicon atom, and the second layer pattern where one of the fluorine atoms adsorbs to a second layer atom and the second fluorine atom adsorbs to a nearby first layer or to another second layer atom. For the SW potential (Table III), the temperature affects the adsorption results. Weber and Stillinger report only three difluorination patterns using a 0 K crystal whereas these results using a 1000 K crystal show five new difluorination patterns: $SiF_2$ formation, second layer sticking by one of the fluorine atoms and patterns shown in Figs. 3(d), 3(f), and 3(i). Since SW only observed three difluorination patterns, where the fluorine atoms adsorb near each other on the surface, they concluded that surface diffusion plays a small role in the adsorption process. According to our results, diffusion still plays a small role, as is evidenced by the production of patterns such as those found in Figs. 3(d), 3(f), and 3(i). The WWC parameterization increases the probability of diffusion a little as evidenced by the new observed difluorination patterns [Figs. 3(e), 3(g), and 3(h)]. For both parameterizations, the Si–F cutoff value is the same, 3.76 Å, thus the increase in the number of diffusion induced patterns using the WWC parameterization must be a result of the increase in the overall attraction of the fluorine atom to the silicon surface.

TABLE II. The number of each pattern of difluorination for the WWC parameterization and the percentage of the trajectories that had nonsimultaneous adsorption. A total of 200 trajectories were performed at each incident energy. See Fig. 3 for the pattern classifications.

| | 0.0195 eV | | 0.234 eV | | 1.67 eV | |
|---|---|---|---|---|---|---|
| Opposing Fig. 3(a) | 25 | 40% | 54 | 28% | 55 | 27% |
| Vicinal Fig. 3(b) | 7 | 17% | 24 | 33% | 53 | 26% |
| Diagonal Fig. 3(c) | 4 | 50% | 11 | 36% | 19 | 37% |
| $SiF_2$ | 4 | 25% | 2 | 0% | 7 | 14% |
| Second layer | 1 | 0% | 3 | 33% | 15 | 40% |
| Figure 3(d) | 2 | 0% | 1 | 100% | 3 | 33% |
| Figure 3(e) | 1 | 100% | 2 | 0% | 11 | 27% |
| Figure 3(f) | 0 | | 3 | 33% | 7 | 0% |
| Figure 3(g) | 0 | | 1 | 100% | 0 | |
| Figure 3(h) | 0 | | 2 | 100% | 0 | |
| Figure 3(i) | 0 | | 0 | | 2 | 100% |
| Total | 44 | 34% | 103 | 32% | 172 | 29% |

TABLE III. The number of each pattern of difluorination for the SW potential and the percentage of the trajectories that had nonsimultaneous adsorption. A total of 200 trajectories were performed at each incident energy. See Fig. 3 for the pattern classifications.

| | 0.0195 eV | | 0.234 eV | | 1.67 eV | |
|---|---|---|---|---|---|---|
| Opposing Fig. 3(a) | 21 | 100% | 27 | 26% | 34 | 100% |
| Vicinal Fig. 3(b), II | 7 | 100% | 13 | 23% | 37 | 84% |
| Diagonal Fig. 3(c) | 2 | 100% | 11 | 18% | 16 | 100% |
| $SiF_2$ | 3 | 100% | 1 | 0% | 10 | 80% |
| Second layer | 0 | | 1 | 0% | 11 | 100% |
| Figure 3(d) | 0 | | 1 | 100% | 1 | 100% |
| Figure 3(e) | 0 | | 0 | | 0 | |
| Figure 3(f) | 1 | 100% | 2 | 100% | 0 | |
| Figure 3(g) | 0 | | 0 | | 0 | |
| Figure 3(h) | 0 | | 0 | | 0 | |
| Figure 3(i),I | 0 | | 1 | 100% | 3 | 67% |
| Total | 34 | 100% | 57 | 28% | 112 | 92% |

Adsorption patterns have been measured for low energy $Cl_2$ adsorption onto Si{001}(2×1).[22] Boland finds that the dominant adsorption patterns are Figs. 3(i) and 3(b), his type I and II respectively, although he does not give the relative contribution of each. This is in contrast to the calculated results in which the opposing adsorption pattern [Fig. 3(a) dominates at low adsorption energies. Without further data it is impossible to ascertain whether this difference is due to deficiencies in the potential, a difference between F and Cl, or equilibration in the experimental data.

In order to investigate the role of time-staggered adsorption in difluorination events, the time between the adsorption of each fluorine atom was calculated. This was accomplished by recording the time in the simulation when the potential energy of each fluorine atom was less than $-5$ eV. Changing

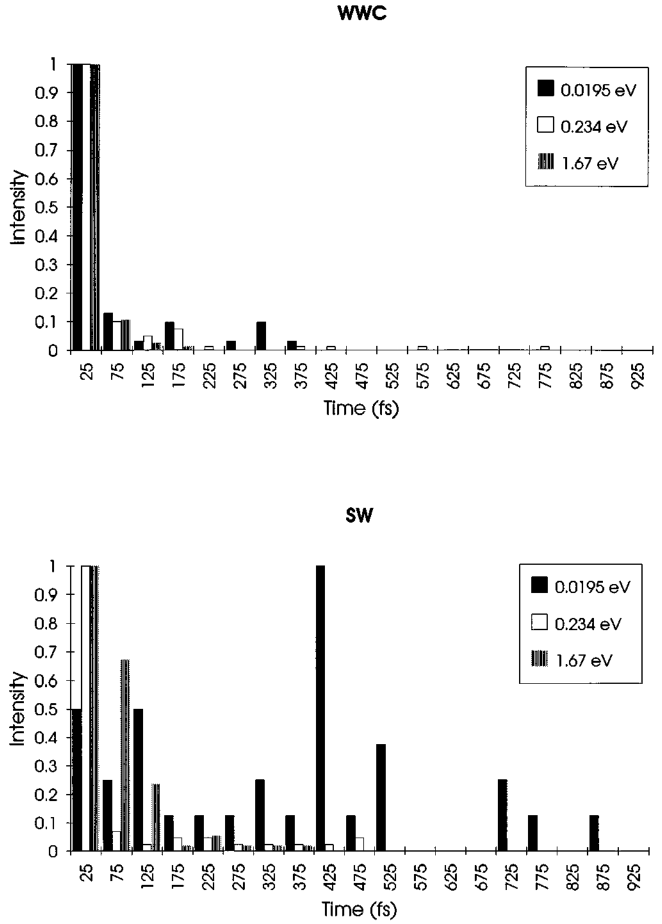

FIG. 4. Distribution of the amount of time between the adsorption of each fluorine atom of the molecule for difluorination events. All distributions are peak normalized.

this criterion to a smaller potential energy does not significantly change the calculated adsorption time difference. Figure 4 shows the distribution of the time differences of difluorination for each initial condition. Regardless of the parameterization, time-staggered adsorption is observed thus giving more indication that *some* molecules adsorb via an atomic precursor mechanism. In addition, the amount of time between the adsorption of the fluorine atoms decreases as the incident kinetic energy of the molecules increases, i.e., more molecules adsorb via the direct adsorption mechanism. This increase in the incident kinetic energy makes a dramatic difference in the distribution of the fluorine atom adsorption time difference using the SW potential and makes little difference using the WWC parameterization. As expected, the WWC parameterization shows fewer overall time-staggered adsorptions than does the SW potential. This time-staggered adsorption mechanism is implied by Carter.[3] While they do not report quantitative results for the amount of time between adsorption events or for the percentage of adsorption events that occur in this manner, they do verify that this mechanism is due to poor placement of the second fluorine atom over low reactivity sites, such as over a Si–Si surface dimer bond.

One interesting question to ponder is the reverse reaction, $F_2$ desorption. Although this is highly improbable given the relative energetics of the Si–F bond strength and the $F_2$ bond strength, such a process does occur for H on Si. Most models for desorption assume that the two H atoms are originally near each other. Given that we observe dissociative adsorption events with the atoms several sites apart, and that there can be relatively long times between the adsorption events, is the reverse process feasible. That is, can one atom attain a precursor position and later find a partner?

Tables II and III detail the percentage of the difluorination trajectories whose fluorine atoms do not adsorb simultaneously, i.e., the difference in the time of adsorption for each fluorine atom is greater than 7.65 fs, which is the arbitrary time increment used to output data during a trajectory. This information shows a dramatic difference between the two parameterizations. In general, nearly all of the difluorination trajectories using the SW potential occur nonsimultaneously, whereas only one-third of those using the WWC parameterization occur nonsimultaneously.

The dependence of difluorination on the initial polar and azimuthal angles of the molecular bond was investigated. Not surprisingly, as the initial kinetic energy of the $F_2$ molecule increases, molecules whose bond axis is perpendicular to the surface are less likely to difluorinate. Conversely, the more parallel the bond axis is to the surface, the more likely the molecule is to difluorinate as the incident kinetic energy increases. The importance of orientation is seen also by Carter and co-workers.[18] All azimuthal angles contribute nearly equally to difluorination for the molecules with the highest incident kinetic energy, whereas at the lowest incident kinetic energy, the azimuthal angles that are closer to being perpendicular to the silicon–silicon surface dimer bond are less likely to difluorinate. For nonsimultaneous difluorination trajectories, there does not appear to be a dependence regarding the molecule's initial polar angle. There is, however, a general trend for there to be more time-staggered adsorption mechanisms for molecules whose bonds are perpendicular to the dimer bond than parallel.

## IV. CONCLUSIONS

Molecular dynamics simulations were performed to investigate how fluorine molecules react with a clean Si{100}(2×1) surface at 1000 K. Stillinger and Weber's (SW) Si–F potential and the Weakliem, Wu and Carter (WWC) reparameterization of the Si–F portion were used. Using the SW potential, the end result of a trajectory is difluorination, monofluorination, repulsion or complex formation, whereas only difluorination or monofluorination are observed using the WWC parameterization. The experiments of Ceyer[5] predict some repulsion in contrast to the predictions using the WWC parameterization. Both the SW potential and the WWC parameterization predict less difluorination than observed by Ceyer. Since this is the most specific piece of experimental data, it is discouraging that both parameterizations of the SW potential fail to predict the high amount of difluorination. In fact, it is not possible from the available experimental data to make a clear determination of which potential is better. Upon analysis of the ejected fluorine atoms of monofluorination events, we find that the adsorption of the first fluorine atom of the diatomic molecule is independent of both the incident kinetic energy and the parameterization. The adsorption of the second fluorine atom, however, is sensitive to these two variables because it can adsorb simultaneously with the first fluorine atom or within an average time of 50 fs, thus via an atomic precursor mechanism. The SW potential predicts more atomic precursor mediated trajectories than the WWC parameterization and the time between adsorption events for the SW potential is longer than for the WWC parameterization. In addition, the WWC parameterization produces a larger variety of diffusion induced difluorination adsorption patterns, providing additional support for the idea of an atomic precursor mediated mechanism for the adsorption of molecular fluorine. It is important to note that these empirical potential energy functions are not fit to the observed time-staggered adsorption mechanism. This mechanism is due to the configuration of the second fluorine atom with the surface once the first fluorine atom has adsorbed. If the second fluorine atom is not close enough to a dangling bond to feel its strong attraction and if it does not possess enough kinetic energy to break its weak attraction to the adsorbed fluorine adatom, time-staggered adsorption/desorption is observed. The results of this article, along with recent hydrogen desorption studies from this same surface, suggest further mechanistic investigations of diatomic adsorption on semiconductor surfaces via experiments and *ab initio* electronic structure calculations need to be performed.

## ACKNOWLEDGMENTS

The authors would like to thank the Office of Naval Research for financial support and The Pennsylvania State University for the generous amount of computer time provided to perform this work. One author (T.A.S.) would like to express her sincerest gratitude to Mike Martys at Gettysburg College for his time and support and to Gettysburg College for computer equipment and time.

[1] T. A. Schoolcraft and B. J. Garrison, J. Vac. Sci. Technol. A **8**, 3496 (1990).
[2] T. A. Weber and F. A. Stillinger, J. Chem. Phys. **92**, 6239 (1990).
[3] L. E. Carter, S. Khodabandeh, P. C. Weakliem, and E. A. Carter, J. Chem. Phys. **100**, 2277 (1994).
[4] J. A. Jensen, C. Yan, E. R. Behringer, and A. C. Kummel, Science **267**, 493 (1995); C. Yan, J. A. Jensen, and A. C. Kummel, J. Chem. Phys. **102**, 3381 (1995).
[5] S. T. Ceyer (private communication). In addition, preliminary values of experimental results have been published in Ref. 3. The authors of this article have used the values given in Ref. 3.
[6] C. T. Rettner, L. A. DeLouise, and D. J. Auerbach, J. Chem. Phys. **85**, 1131 (1986).
[7] B. I. Craig and P. V. Smith, Surf. Sci. **239**, 36 (1990).
[8] K. Sinniah, M. G. Sherman, L. B. Lewis, W. H. Weinberg, J. T. Yates, Jr., and J. C. Janda, Phys. Rev. Lett. **62**, 567 (1989); J. Chem. Phys. **92**, 5700 (1990).
[9] M. L. Wise, B. G. Koehler, P. Gupta, P. A. Coon, and S. M. George, Surf. Sci. **258**, 166 (1991).
[10] J. J. Boland, Phys. Rev. Lett. **67**, 1539 (1991); J. Vac. Sci. Technol. A **10**, 2458 (1992).
[11] M. P. D'Evelyn, Y. L. Yang, and L. F. Sutcu, J. Chem. Phys. **96**, 852 (1992).
[12] S. F. Shane, K. W. Kolasinski, and R. N. Zare, J. Chem. Phys. **97**, 3704 (1992).
[13] F. H. Stillinger and T. Weber, Phys. Rev. B **31**, 5262 (1985).
[14] F. H. Stillinger and T. Weber, J. Chem. Phys. **88**, 5123 (1988).
[15] F. H. Stillinger and T. Weber, Phys. Rev. Lett. **62**, 2144 (1989).
[16] P. C. Weakliem, C. J. Wu, and E. A. Carter, Phys. Rev. Lett. **69**, 200 (1992); erratum *ibid.* **69**, 1475 (1992).
[17] P. C. Weakliem and E. A. Carter, J. Chem. Phys. **98**, 737 (1993).
[18] L. E. Carter and E. A. Carter, J. Vac. Sci. Technol. A **12**, 2235 (1994).
[19] T. A. Schoolcraft and B. J. Garrison, J. Am. Chem. Soc. **113**, 8221 (1991).
[20] M. Karplus, R. N. Porter, and R. D. Sharma, J. Chem. Phys. **43**, 3259 (1965).
[21] J. R. Engstrom, M. M. Nelson, and T. Engel, Surf. Sci. **215**, 437 (1989).
[22] J. J. Boland, Science **262**, 1703 (1993).